

## DIFFUSE X-RAYS IN THE GALACTIC CENTER REGION — THE ZOO OF IRON LINE CLUMPS, NON-THERMAL FILAMENTS AND HOT PLASMAS —

**Aya Bamba<sup>1</sup>, Hiroshi Murakami<sup>1</sup>, Atsushi Senda<sup>1</sup>, Shin-ichiro Takagi<sup>1</sup>, Jun Yokogawa<sup>1</sup>, and Katsuji Koyama<sup>1</sup>**

Department of Physics, Graduate School of Science, Kyoto University, Kita-shirakawa, Sakyo-ku, Kyoto, 606-8502, Japan

### ABSTRACT

This paper reports the diffuse X-ray features around the Galactic center observed with *Chandra*. We confirm the *ASCA* and *Ginga* discoveries of the large-scale thin-thermal plasma with strong lines in the Galactic center region. In addition, many small clumps of emission lines from neutral (6.4 keV line) to He-like (6.7 keV line) irons are discovered. The 6.4 keV line clumps would be reflection nebulae, while those of the 6.7 keV line are likely SNRs. We also find emission lines of intermediate energy between 6.5–6.7 keV, which are attributable to young SNRs in non equilibrium ionization. Non-thermal filaments or belts with X-ray spectra of no emission line are found, suggesting the Fermi acceleration site in a rapidly expanding shell. All these suggest that multiple-supernovae or extremely large explosion had occurred around the Galactic center region in the recent past.

**Key words:** Galaxy: center — reflection nebulae — supernova remnants — acceleration of particles

### 1. INTRODUCTION

In the Galactic center (GC) region, *Ginga* and *ASCA* found the large-scale thin-thermal plasma with highly ionized atomic lines (Koyama et al. 1989). On the other hand, Murakami et al. (2000; 2001a; 2001b) discovered clumps with a neutral iron line and proposed the X-ray reflection nebulae (XRNe) scenario. Clumps of highly ionized iron line are also discovered with *Chandra* and are inferred to be young SNRs (e.g. Senda et al. 2002).

In this paper, we report on new diffuse X-ray structures around the Galactic center Sgr A\*, the molecular cloud Sgr B2 and Sgr C, and the Radio Arc regions revealed with the excellent spatial resolution of *Chandra* and summarize their characteristics.

### 2. OBSERVATIONS

We use the *Chandra* archive data of the ACIS-I array on the Radio Arc, Sgr A\*, Sgr B2, and Sgr C regions. The field of view (FOV) of each observation is  $17' \times 17'$ . The on-axis position ( $l, b$ ) and exposure time are given in Table 1.

*Table 1.* The on-axis position and exposure time in each observation.

| Region    | On-axis Position ( $l, b$ ) | Exposure [ksec] |
|-----------|-----------------------------|-----------------|
| Sgr A*    | (359°.94, -0°.04)           | 46              |
| Sgr B2    | (0°.59, -0°.02)             | 99              |
| Sgr C     | (359°.41, -0°.00)           | 20              |
| Radio Arc | (0°.4, -0°.01)              | 49              |

### 3. DATA ANALYSES AND RESULTS

Figure 1 shows the 3.0–8.0 keV band images around Sgr B2 (Figure 1a), Radio Arc and Sgr A\* (mosaic; Figure 1b), and Sgr C (Figure 1c). Many diffuse or filamentary structures (No 1–20 indicated in Figure 1) are found.

We performed the spectral fitting for all the diffuse sources (No 1–20). Background spectra were taken from around each source. The background-subtracted spectra were fitted with a model of power-law continuum plus a narrow Gaussian line. Then we classified all clumps by the best-fit line profile; 6.4 keV line clumps, 6.5–6.7 keV line clumps, and clumps with no significant line. The fitting results are separately given in Table 2 (a, b, and c).

### 4. DISCUSSIONS

#### 4.1. THE 6.4 keV LINE CLUMPS

Most of the 6.4 keV line clumps show deep absorptions in excess to that toward the GC region, similar to the XRN, Sgr B2 (Murakami et al. 2000). They hence are regarded as new XRN candidates.

Figure 2 is the 6.0–7.0 keV image around Sgr C superposed on the CS J=1–0 contours (Tsuboi et al. 1999). The spectrum of Sgr C shows the neutral iron line and deep absorption. The iron line emission is shifted toward the GC side of the molecular cloud, as is found for the first XRN, Sgr B2. Therefore, we fitted the spectrum of Sgr C region with an XRN model. Since the statistics is limited, we fixed the photon index to 2.0 (Murakami et al. 2000) and the equivalent width of the 6.4 keV line to 2.0 keV (Inoue 1985), expected value for XRNe. The fitting is acceptable with the best-fit parameters shown in Table 2. Thus, we confirmed the *ASCA* result that Sgr C is an XRN (Murakami et al. 2001a).

Table 2. Best-fit parameters of the 6.4 keV (a), 6.5–6.7 keV (b), and line-less (c) clumps.

| Source No.                          | $\Gamma$        | Center Energy<br>[keV] | Equivalent Width<br>[keV] | $N_{\text{H}}$<br>[ $\times 10^{22} \text{ cm}^{-2}$ ] | Flux (2–10 keV)*<br>[ergs $\text{cm}^{-2} \text{s}^{-1}$ ] |
|-------------------------------------|-----------------|------------------------|---------------------------|--|--|
| <hr/>                               |                 |                        |                           |  |  |
| — (a) The 6.4 keV line clumps —     |                 |                        |                           |  |  |
| 3                                   | 1.8 (−1.0–5.8)  | 6.34 (6.26–6.41)       | 0.9 (0.5–1.3)             | 33 (17–51)   | $1.2 \times 10^{-12}$                                      |
| 5                                   | 0.5 (−0.6–1.1)  | 6.43 (6.37–6.55)       | 1.3 (0.8–1.8)             | 4 (1–10)   | $7.2 \times 10^{-13}$                                      |
| 6                                   | 1.6 (−0.7–6.6)  | 6.35 (6.29–6.41)       | 1.6 (0.8–2.4)             | 12 (3–30)  | $4.6 \times 10^{-13}$                                      |
| 7                                   | 3.5 (2.0–4.5)   | 5.97 (5.85–6.42)       | 1.1 (0.6–2.4)             | 8 (5–12)   | $4.9 \times 10^{-13}$                                      |
| 9                                   | −0.1 (−1.1–1.3) | 6.41 (6.36–6.45)       | 0.8 (0.5–1.1)             | 10 (2–27)  | $1.1 \times 10^{-12}$                                      |
| 13                                  | 1.0 (0.2–1.7)   | 6.41 (6.37–6.45)       | 1.7 (0.3–88)              | 40 (20–63)   | $6.6 \times 10^{-13}$                                      |
| 14                                  | 0.7 (−2.0–4.6)  | 6.42 (6.38–6.47)       | 1.9 (> 0.08)              | 20 (12–43)   | $4.1 \times 10^{-13}$                                      |
| 15 (Sgr C) <sup>†</sup>             | 2.0(fixed)      | 6.36 (6.08–6.44)       | 2 (fixed)                 | 16 (9–34)  | $9.1 \times 10^{-13}$                                      |
| 16                                  | 2.7 (1.6–3.7)   | 6.42 (5.62–7.94)       | 1.4 (0.7–2.7)             | 7 (4–12)   | $1.5 \times 10^{-12}$                                      |
| 17                                  | 7.3 (>2.6)      | 6.46 (not determined)  | 1.8 (< 5.0)               | 41 (12–67)   | $8.4 \times 10^{-12}$                                      |
| 19                                  | 3.7 (0.5–9.1)   | 6.37 (6.30–6.40)       | 1.4 (0.8–2.63)            | 34 (17–78)   | $2.5 \times 10^{-12}$                                      |
| 20 (Arches) <sup>‡</sup>            | 5.0 (>2.0)      | 6.38 (6.34–6.42)       | 1.7(0.9–2.2)              | 34 (13–59)   | $5.0 \times 10^{-12}$                                      |
| <hr/>                               |                 |                        |                           |  |  |
| — (b) The 6.5–6.7 keV line clumps — |                 |                        |                           |  |  |
| 1                                   | 3.9 (2.2–7.1)   | 6.64 (6.52–6.88)       | 0.5 (0.1–1.2)             | 57 (38–71)   | $5.7 \times 10^{-12}$                                      |
| 8                                   | 1.9 (0.3–4.3)   | 6.83 (6.63–7.01)       | 2.6 (0.4–4.6)             | 4 (2–12)   | $1.6 \times 10^{-13}$                                      |
| 12                                  | 9.4 (> 5.8)     | 6.62 (6.58–6.63)       | 19 (> 6.6)                | 44 (21–52)   | $3.5 \times 10^{-13}$                                      |
| 18                                  | 3.5 (2.5–4.5)   | 6.70 (6.56–6.83)       | 2.3 (1.0–3.6)             | 8 (6–11)   | $9.5 \times 10^{-13}$                                      |
| <hr/>                               |                 |                        |                           |  |  |
| — (c) The line-less clumps —        |                 |                        |                           |  |  |
| 2                                   | 2.5 (1.3–4.5)   | —                      | —                         | 11 (7–21)  | $2.9 \times 10^{-13}$                                      |
| 4                                   | 2.5 (0.8–5.0)   | —                      | —                         | 7 (3–18)   | $1.1 \times 10^{-13}$                                      |
| 10                                  | 1.0 (−0.9–6.5)  | —                      | —                         | 2 (< 15)   | $5.9 \times 10^{-14}$                                      |
| 11                                  | 1.3 (0.8–2.0)   | —                      | —                         | 6 (3–9)  | $4.7 \times 10^{-13}$                                      |

Parentheses indicate 90% confidence regions for one relevant parameter.

\*: Absorption corrected flux

<sup>†</sup>: Parameters are determined with an XRN model (see text)

<sup>‡</sup>: Diffuse emission near the Arches cluster (see text)

*ASCA* found the 6.4 keV line emission near at the molecular cloud CO 0.13–0.13 (Koyama et al. 1996, Tsuboi et al. 1999). The *Chandra* observations revealed the X-ray structure has two clumps of No 9 and 10. The 6.4 keV lines are mainly coming from No 9, a filament lying along the southwest half of the cloud, hence may be fluorescence irradiated by a GC side source.

Another candidate of XRN, but may be unrelated to Sgr A\* is an  $1' \times 2'$ -ellipse located near the active star forming region, the Arches cluster at a distance of 8.5 kpc (Nagata et al. 1995). The spectral parameters show a strong neutral iron line and deep absorption, supporting the XRN scenario. The irradiating sources, however are likely active young stars in the Arches cluster (Yusef-Zadeh et al. 2001). We find three X-ray bright stars with the total luminosity of a few  $\times 10^{34}$  ergs  $\text{s}^{-1}$ , assuming a single temperature plasma. However the required luminosity to produce the diffuse 6.4 keV flux is a few  $\times 10^{35}$  ergs  $\text{s}^{-1}$ , 10 times larger than that of the core stars. Since X-rays from young stars are more active and variable in younger age, it is conceivable that big flares and/or bursts were more frequently occurred in the recent past than in the present.

The other 6.4 keV clumps No 3, 5–7 are located in between Sgr A\* and the Radio Arc, and show no clear association with molecular clouds. Hence the origin of these sources is puzzling.

#### 4.2. THE 6.5–6.7 KEV LINE CLUMPS

Since the 6.5–6.7 keV line comes from highly ionized iron, we can infer that these clumps consist of hot plasmas. An X-ray shell No 1 is associated with a non-thermal radio source “wisp” (Ho et al. 1985), suggesting to be a part of the radio SNR, G359.92–0.09 (Coil & Ho 2000). In fact, we see diffuse X-rays filling in the east half of G359.92–0.09 (dotted circle in Figure 1b), while the west half including No 1 may be behind the molecular cloud M–0.13–0.08, hence is faint and/or largely absorbed in X-ray. The X-ray spectrum is well fitted with an NEI model of a temperature  $> 3$  keV, significantly higher than any other young SNRs, but comparable to the diffuse emission prevailing in the whole GC region. Together with the *Chandra* discovery of new X-ray SNRs, Sgr A East (Maeda et al. 2002) and G0.570–0.018 (Senda et al. 2002), we suspect that many other young X-ray SNRs would be

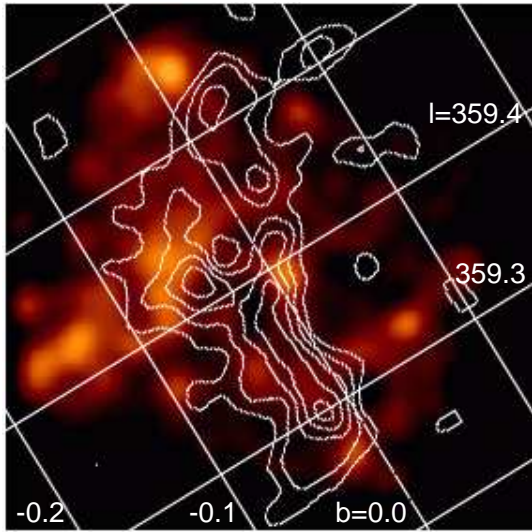


Figure 2. The mosaic 6.0–7.0 keV image around the Sgr C region with the Galactic coordinate (solid lines). White contours represent the radio fluxes of the CS  $J=1-0$  transition line. The north is up and the east is left.

found in the further deep observations. These putative SNRs may significantly contribute to the large scale diffuse X-rays near the GC.

No 18 has a plume-like shape lying at the northwest of Sgr A\* and perpendicular to the Galactic plane. The plasma temperature is lower than that in the GC. This source may not be a single SNR but is likely to be an outflow from the GC plasma. An attractive idea is that No 18 is a thermal jet emanating from the giant black hole Sgr A\*.

#### 4.3. THE LINE-LESS CLUMPS

The presence of Non-thermal radio filaments is one of the most striking features in the GC region. They are all oriented perpendicular to the Galactic plane, and are considered to be synchrotron emission in a strong magnetic field of  $\sim 1\text{mG}$ . *Chandra* discovered non-thermal X-ray filaments from Sgr A East (No 2) and near the Radio Arc (No 10) (Koyama 2001). A hint of possible association with a weak radio filament is suggested for these X-ray filaments. We thus infer that the X-ray filaments are due either to the synchrotron emission or Inverse Compton in a relatively weak magnetic field, where the radio flux is rather faint.

Since No 10 is located at the east rim of the molecular cloud CO 0.13–0.13, where the expanding cavity is interacting with the cloud (Oka et al. 2001), the Fermi acceleration scenario is likely to produce high energy electrons. The synchrotron energy loss of high energy electrons may not be large, hence can emit even synchrotron X-rays. If the magnetic field is moderately weak, X-rays are more

likely from the Inverse Compton process as proposed for the X-ray filament at the radio "Thread" G 359.54+0.18 (Wang et al. 2002).

No 11 is a faint X-ray belt running parallel to the Galactic plane and probably extending to the other non-thermal filament No 4.

#### 5. SUMMARY

1. Many diffuse X-ray clumps with different morphology are found from the GC region.
2. The X-ray spectra are full of variety in line feature: iron lines of 6.4 keV, 6.5–6.7 keV, and line-less clumps.
3. The molecular clouds Sgr C and CO0.13–0.13 are likely XRNe, irradiated by the past active Sgr A\* (Murakami et al. 2001b). The diffuse 6.4 keV X-rays near the Arches cluster would be due to the irradiating of flaring young stars in the cluster.
4. Some of the other 6.4 keV clumps located in between Sgr A\* and the Radio Arc regions show no clear association with molecular clouds, hence the origin is debatable.
5. The 6.5–6.7 keV clumps may be young SNRs, but the temperatures are higher than the usual SNRs.
6. The line-less clumps (filaments) would be either synchrotron or Inverse Compton X-rays in weaker magnetic field than those in the radio bright filaments.

#### REFERENCES

- Coil A.L., Ho P.T.P. 2000, ApJ, 533, 245  
 Inoue H. 1985, Space Science Review, 40, 317  
 Koyama K., Awaki H., Kunieda H., Takano S., Tawara Y. 1989, Nature, 339, 603  
 Koyama K., Maeda Y., Sonobe Y., Takeshima T., Tanaka Y., Yamauchi S. 1996 PASJ, 48, 249  
 Koyama. K. 2001, "New Century of X-ray Astronomy", ASP Conference Series, Vol. 251, 50, eds. H. Inoue and H. Kunieda, astroph/0108109  
 Ho P.T.P., Jackson J.M., Barrett A.H., Armstrong, J.T. 1985, ApJ, 288, 575  
 Maeda Y., Baganoff F.K., Feigelson E.D., Morris M., Bautz M.W., Brandt W.N., Burrows D.N., Doty J.P. et al. accepted by ApJ, astroph/0102183  
 Murakami H., Koyama K., Sakano M., Tsujimoto M., Maeda Y. 2000, ApJ, 534, 283  
 Murakami H., Koyama K., Tsujimoto M., Maeda Y., Sakano M. 2001a, ApJ, 550, 297  
 Murakami H., Koyama K., Maeda Y. 2001b, ApJ, 558, 687  
 Nagata T., Woodward C.E., Shure M., Kobayashi N. 1995, AJ, 109, 1676  
 Oka T., Hasegawa, T., Sato, F., Tsuboi, M., Miyazaki, A. 2001, PASJ, 53, 779  
 Senda A., Murakami H., Koyama K. 2002, accepted by ApJ, astroph/0110011  
 Tsuboi M., Handa T., Ukita N. 1999, ApJS, 120, 1  
 Wang Q.D., Gotthelf E.V. Lang C.C. 2002, accepted by Nature, astroph/0201070

Yusef-Zadeh F., Law C., Wardle M., Wang Q.D., Fruscione A.,  
Lang C.C., Cotera A. 2001, *astroph/0108174*

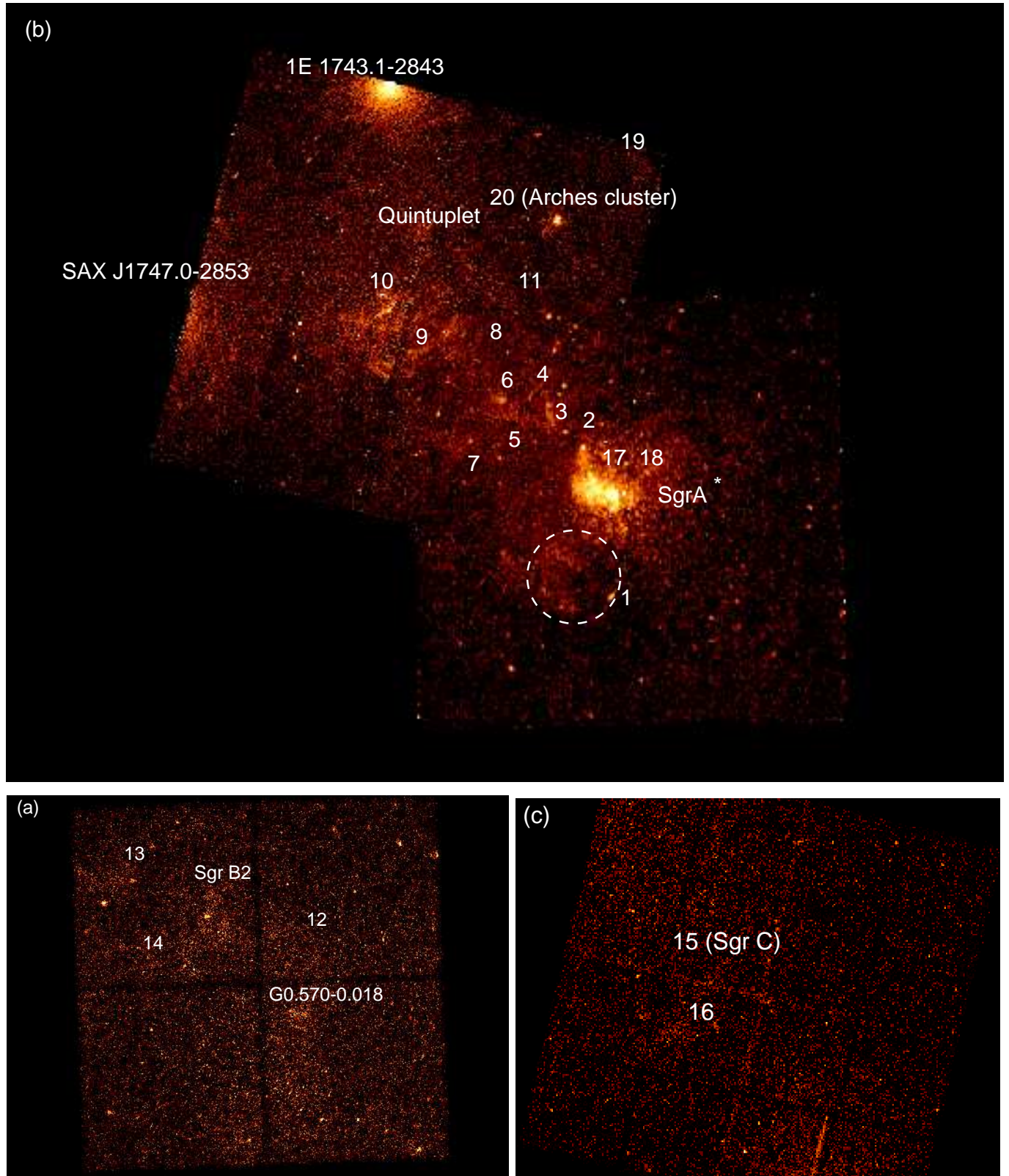


*Figure 1.* The 3.0–8.0 keV band images in the Radio Arc and Sgr A\* regions (mosaic; a), Sgr B2 (b) and Sgr C (c) regions. The north is up and the east is left. The diffuse clumps are shown with numbers 1–20. The dashed circle indicates the radio SNR G359.92–0.09.